Application of Statistical Physics to Understand Static and Dynamic Anomalies in Liquid Water[1]

**H. E. Stanley,[2] S. V. Buldyrev,[2] N. Giovambattista,[2] E. La Nave,[2, 3]
S. Mossa,[2] A. Scala,[2, 3] F. Sciortino,[3] F. W. Starr,[4] and M. Yamada[2]**

We present an overview of recent research applying ideas of statistical mechanics to try to better understand the statics and especially the dynamic puzzles regarding liquid water. We discuss recent molecular dynamics simulations using the Mahoney–Jorgensen transferable intermolecular potential with five points (TIP5P), which is closer to real water than previously-proposed classical pairwise additive potentials. Simulations of the TIP5P model for a wide range of deeply supercooled states, including both positive and negative pressures, reveal (i) the existence of a non-monotonic temperature of maximum density line and a non-reentrant spinodal, (ii) the presence of a low-temperature phase transition. The take-home message for the static aspects is that what seems to "matter" more than previously appreciated is local tetrahedral order, so that liquid water has features in common with SiO_2 and P, as well as perhaps Si and C. To better understand dynamic aspects of water, we focus on the role of the number of *diffusive* directions in the potential energy landscape. What seems to "matter" most is not values of thermodynamic parameters such as temperature T and pressure P, but only the value of a parameter characterizing the potential energy landscape—just as near a critical point what matters is not the values of T and P but rather the values of the correlation length.

[2] Center for Polymer Studies and Department of Physics, Boston University, Boston, Massachusetts 02215; e-mail: hes@meta.bu.edu

[3] Dipartimento di Fisica Università di Roma La Sapienza, Istituto Nazionale di Fisica della Materia and INFM Center for Statistical Mechanics and Complexity, Piazzale Aldo Moro 2, 00185 Roma, Italy.

[4] Polymers Division and Center for Theoretical and Computational Materials Science, National Institute of Standards and Technology, Gaithersburg, Maryland 20899.

1. THE GOAL: UNDERSTANDING ''WHAT MATTERS''

Many physicists are attracted to physics because of the focus on understanding just enough of a subject to comprehend the key features that really matter. As soon as some physicists feel they understand ''what matters,'' insatiable appetites for novelty force attention to new puzzles. Among most exciting new developments in the 1960's (when the first author met Michael Fisher) was the degree to which the principle of scale invariance provided increased understanding of ''what matters'' near a critical point. The key point was that what matters near a critical point is the correlation length for statics, and the correlation time for dynamics. An exciting question these days is ''what matters'' in understanding the statics and dynamics of liquid water, and important clues are emerging when one focuses on behavior in the deeply supercooled region, especially just above —and just below—the "critical" temperature T_{MCT} predicted by mode coupling theory.

2. STATICS: ''WHAT MATTERS'' IS LOCAL TETRAHEDRAL GEOMETRY

2.1. Introduction

Liquid water is not a typical liquid. However, some progress has occurred in understanding its highly anomalous equilibrium and dynamical properties.[1–6] Water is a space-filling hydrogen bond network, as expected from continuum models of water. However when we focus on the well-bonded molecules, we find that water can be regarded as having certain clustering features—the clusters being not isolated ''icebergs'' in a sea of dissociated liquid (as postulated in mixture models dating back to Röntgen) but rather patches of well-bonded molecules embedded in a highly connected network or "transient gel."[7–10] Similar physical reasoning applies if we generalize the concept of well-bonded molecules to molecules with a smaller than average energy[11] or to molecules with a more ordered than average "local structure".[12]

2.2. Liquid–Liquid Phase Transition Hypothesis

Poole et al made computer simulations of the ST2 model of water, with the goal of exploring in detail what might happen in the low-temperature region,[13] and discovered in this artificial ''computer water'' the existence of a second critical point C', below which the liquid phase separates into two distinct phases—a low-density liquid (LDL) and a high-density

liquid (HDL). It is not required that the system is exactly *at* its critical point for the system to exhibit remarkable behavior, such as the phenomenon of critical opalescence discovered and correctly explained in 1869 by Andrews[14] in terms of increased fluctuations away from (but close to) the critical point. Thus, although in experiments one cannot get closer than $(5-15)°$, C' nonetheless exerts a strong effect in the experimentally-accessible region of the phase diagram. If we have a singularity in our phase diagram at a well-defined critical point, it's going to have an effect on an entire region around it—a "critical region."

2.3. Experimental Work

When liquid water is supercooled below the homogeneous nucleation temperature T_H ($-38°C$ at $P = 1$ atm), crystal phases nucleate homogeneously, and the liquid freezes spontaneously to the crystalline phase. Mishima creates 1 cm^3 high-pressure ices in a piston-cylinder apparatus, decompresses the sample at a constant rate of 0.2 GPa/min, and—because melting is endothermic—observes melting transitions of the ice polymorphs using a thermocouple to detect a change in the sample temperature during the decompression.[15, 16] He then determines melting pressures at different temperatures. The melting curves he obtains agree with previously-reported data for stable melting lines,[17, 18] and extend our knowledge of the location of metastable melting lines to much lower temperatures.

The Gibbs potential G of the ice polymorphs is known. Since G is identical in coexisting phases, locating the melting lines of the ice polymorphs is sufficient to learn G for water along these lines. By interpolating data for G obtained along these melting lines, one can find the approximate experimental G for a wide range of temperatures and pressures in the no-man's land below T_H.[15] After finding G as a function of pressure P and temperature T, one can find by differentiation the volume as a function of P and T. Volume as a function of T is just what we want—this is the equation of state of liquid water. The P-V-T relation found is consistent with the existence of a line of first-order liquid–liquid transitions which continues from the line of low-density amorphous—high-density amorphous transitions and terminates at an apparent critical point C'. The P-V-T relation is also consistent with other known experimental data[19–25] and also with a number of theoretical and simulation results.[12, 13, 26–35]

2.4. Theoretical Work

The most natural response to the concept of a second critical point in a liquid is bafflement—such a thing just does not make sense. To make the

concept more plausible, we offer the following remarks. Consider a typical member of the class of intermolecular potentials that go by the name of core-softened potentials.[36–38] Recently such potentials have been revisited;[27, 39–52] they are attractive to study because they can be solved analytically in one-dimension and are tractable to study using approximation procedures (and simulations) in higher dimensions. They are also more realistic than one might imagine at first sight, and indeed may reflect "what matters" in water-water interactions, since the repulsive soft core mimics the effect of the small number (four) of nearest neighbors in liquids with a local tetrahedral structure. Although such a picture may seem to be oversimplified, it is consistent with neutron data.[21–24] Also, simulation results are in good accord with neutron results (see, e.g., ref. 53), and Sasai relates these two distinct local structures to dynamic properties.[54]

2.5. Simulations

The shape of the spinodal in the negative-pressure region can be used to test the liquid–liquid phase transition hypothesis, so we briefly discuss recent calculations of the density and pressure of the spinodal, which we denote $\rho_{sp}(T)$ and $P_{sp}(T)$, respectively. Relatively few experimental works[55, 56] and simulations[13, 57–61] have been performed on "stretched" water. Recently, Yamada and her coworkers[30] simulated a system of $N = 343$ molecules interacting with the TIP5P potential.[62] TIP5P is a five-site, rigid, non-polarizable water model, not unlike the ST2 model.[63] The TIP5P potential accurately reproduces the density anomaly at 1 atm and exhibits excellent structural properties when compared with experimental data.[62, 64] The TMD shows the correct pressure dependence, shifting to lower temperatures as pressure is increased. Under ambient conditions, the diffusion constant is close to the experimental value, with reasonable temperature and pressure dependence away from ambient conditions.[62]

Figure 1 shows results for pressure along isotherms. At lower temperatures an inflection develops, which becomes a "flat" isotherm at the lowest temperature, $T = 215$ K. The presence of a flat region indicates that a phase separation takes place; the critical temperature is $T_{C'} = (217 \pm 3)$ K, the critical pressure is $P_{C'} = (340 \pm 20)$ MPa, and the critical density $\rho_{C'} = (1.13 \pm 0.04)$ g/cm^3.

Figure 2 plots the pressure along isochores. The curves show minima as a function of temperature; the locus of the minima is the TMD line, since $(\partial P/\partial T)_V = \alpha_P/K_T$, the ratio of the thermal expansivity to isothermal compressibility. Note that the pressure exhibits a minimum if the density passes through a maximum ($\alpha_P = 0$). It is clear that, as in the case of ST2
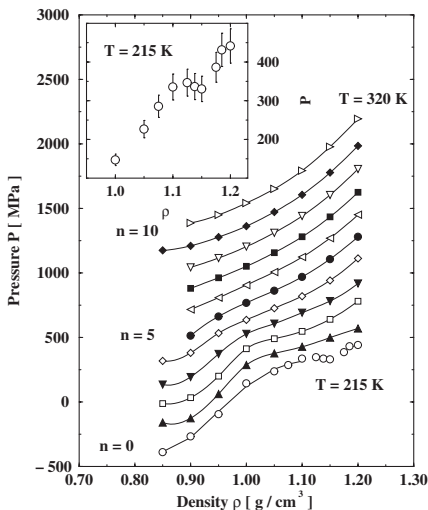
Fig. 1. Dependence on density of the pressure at all temperatures investigated ($T =$ [215, 220, 230, 240, 250, 260, 270, 280, 290, 300, 320] K, from bottom to top). Each curve has been shifted by $n \times 150$ MPa to avoid overlaps. An inflection appears as T is decreased, transforming into a "flat" coexistence region at $T = 215$ K, indicating the presence of a liquid–liquid transition. Inset: A detailed view of the $T = 215$ K isotherm. Courtesy of M. Yamada.

water, TIP5P water has a TMD that changes slope from negative to positive as P decreases. Notably, the point of crossover between the two behaviors is located at ambient pressure, $T \approx 4°C$, and $\rho \approx 1$ g/cm^3. Also plotted is the spinodal line, obtained by fitting the isotherms (for $T \geqslant 300$ K) of Fig. 1 to the form $P(T, \rho) = P_s(T) + A[\rho - \rho_s(T)]^2$, where $P_s(T)$ and
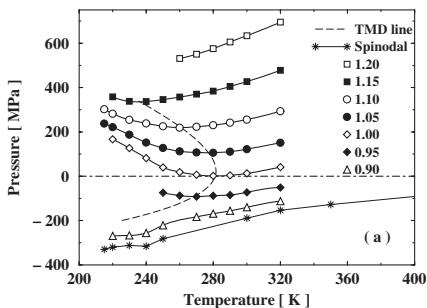

Fig. 2. Pressure along seven isochores of density (0.90, 0.95,..., 1.20) g/cm^3. The minima correspond to the temperature of maximum density line (dashed line). Note the "nose" of the TMD line at $T = 4°C$. Stars denote the liquid spinodal line, which is not reentrant, and terminates at the liquid-gas critical point. Courtesy of M. Yamada.

$\rho_s(T)$ denote the pressure and density of the spinodal line. This functional form is the mean field prediction for $P(\rho)$ close to a spinodal line. For $T \leqslant 250 K$, $P_s(T)$ is calculated by estimating the location of the minimum of $P(\rho)$. The results in Fig. 2 show that the liquid spinodal line is not reentrant and does not intersect the TMD line.

2.6. Outlook

Before concluding this brief discussion of statics, we ask ''What is the requirement for a liquid to display a liquid–liquid phase transition?'' By the arguments presented above, some other liquids should display liquid–liquid phase transitions, namely systems that at low temperature and low pressure have anticorrelated entropy and specific volume fluctuations. Thus a natural extension to our work is to consider other tetrahedrally-coordinated liquids. Since other tetrahedral liquids have that similar features, we might anticipate similar liquid–liquid phase transitions occur on the liquid free energy surface of these liquids. Evidence in favor of this possibility has been reported for SiO_2,[66, 67] amorphous GaSb,[68, 69] C,[70, 71] and Si.[72] Recently, clear experimental evidence for a liquid–liquid phase transition has been reported in phosphorus, where the low-density liquid phase is a molecular liquid of tetrahedral P_4 ''molecules.''[73, 74] With a change in pressure, the low-pressure, low-density molecular liquid transforms to a high-pressure, high-density polymeric liquid. During the transformation, two forms of liquid coexist, showing that phosphorus has a first-order liquid–liquid phase transition.[75] A careful analysis of tetrahedral liquids with and without liquid–liquid phase transitions has recently been published,[76] who compares the density maxima of the four best researched examples of tetrahedral liquids (SiO_2, BeF_2, H_2O, and liquid Si), compares their special liquid state heat capacity behavior, and places them in a semi-quantitative relationship in their anomalous transport properties.

3. DYNAMICS ON THE POTENTIAL ENERGY LANDSCAPE: ''WHAT MATTERS'' IS THE NUMBER OF DIFFUSIVE DIRECTIONS

3.1. Introduction

The study of the dynamics in supercooled liquids is receiving great interest[77] due to novel experimental techniques,[78, 79] detailed theoretical predictions,[80] and by the opportunity to follow the microscopic dynamics via computer simulation.[81, 82] Mode coupling theory[80] quantitatively predicts the time evolution of correlation functions and the dependence on

temperature T of characteristic correlation times. Unfortunately, the temperature region in which mode coupling theory is able to make such predictions for the long time dynamics is limited to weakly supercooled states. Parallel with the development of mode coupling theory, theoretical work[83–87] has called attention to thermodynamic approaches to the glass transition, and to the role of configurational entropy in the slowing down of dynamics.[88–90] These theories, which build on ideas put forward some time ago,[91–93] stress the relevance of the topology of the potential energy landscape explored in supercooled states. Detailed studies of the potential energy landscape may provide insights into the slow dynamics of liquids, and new ideas for extending the present theories to the deep supercooling regime.

3.2. Instantaneous Normal Modes and the Topology of the Potential Energy Landscape

One approach to understanding the role of the potential energy landscape is to study the connectivity between different local configurations using the instantaneous normal mode formalism.[94] Analogous to the standard normal mode theory for solids, an instantaneous normal mode is the eigenfunction of the Hessian, which is the matrix of the second derivatives of the potential energy with respect to all 6N atomic coordinates. In a liquid state, the eigenvalues of the Hessian matrix are not all generally positive; the negative eigenvalues indicate a downward curvature of the potential energy landscape, i.e., indicate unstable directions for the system. Previous studies using the instantaneous normal mode formalism indicate that the number of directions with negative curvature is reduced on cooling, motivating theories relating diffusion in liquids to the instantaneous normal mode density of states.[95, 96] Low temperature liquid dynamics involve the superposition of fast oscillations around quasi-equilibrium positions (intra-basin motion) and the rearrangement of the system between these positions (inter-basin motion). The typical oscillation period is much shorter than the typical time needed by the system to rearrange itself, i.e., the structural relaxation time. instantaneous normal mode theories for diffusion relate the diffusion of the system in configuration space to activated processes of inter-basin motion. In this respect, the unstable modes are considered representative of the barriers crossed when the system changes basins.

One approach[97, 98] among many[99, 100] for separating the diffusive modes (basin changes in configuration space) from the non-diffusive modes (no basin changes) is classifying the modes according to their potential energy profile (Fig. 3), and partition those unstable modes into two groups:
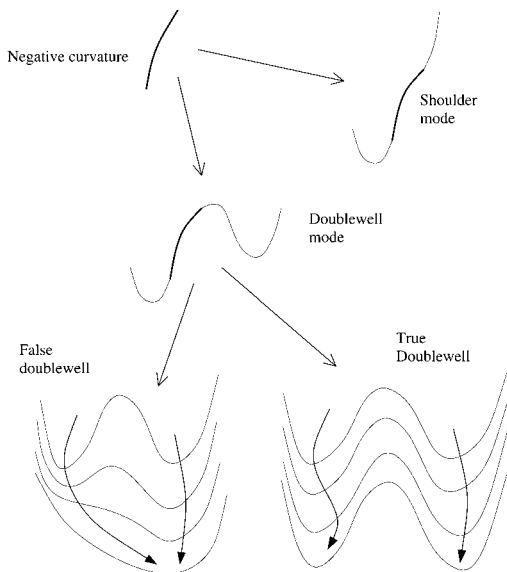
Fig. 3. Schematic sketch of the possible shapes of the potential energy landscape associated with imaginary eigenvalues. Unstable modes are first separated into shoulder and double well modes. Furthermore, double well modes are split into diffusive and non diffusive ones. Courtesy of E. LaNave.

(i) unstable normal modes due to the anharmonicities (shoulder modes) and (ii) modes along which the system is crossing a saddle (double-well modes).[99] In order to distinguish between shoulder and double-well modes, the potential energy profile is calculated along straight paths that follow the direction of the eigenvector. Furthermore, to distinguish the false and true double wells, we calculate the steepest descent trajectories starting from the opposite sides of the saddle. A mode represents true double well, and this is called a diffusive mode if these trajectories end up in two distinct local minima.

3.3. Results

Next we discuss the numerical relationship between D and the number of diffusive modes f_{diff} in the vicinity of the fragile-to-strong crossover temperature $T_\times$. We review recent work on two different models of tetrahedral liquids, the SPC/E extended simple point charge model for water[98, 101] and the BKS model of silica.[102] For silica (Fig. 4), the fragile-to-strong transition temperature $T_\times$ coincides numerically[102–105] with the critical temperature T_{MCT} identified by mode coupling theory. For both models, it appears that D depends on T and P only through f_{diff}—the
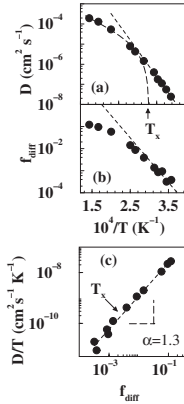
Fig. 4. Arrhenius plot of (a) the diffusion constant D for Si atoms in SiO_2 and (b) f_{diff}. The crossover to the straight line Arrhenius behavior below $T_\times$ represents the fragile-to-strong crossover for silica. Part (c) shows the parametric relation D/T vs f_{diff} in a log-log scale. The data are smooth through the "mode-coupling" crossover temperature $T_\times$. Courtesy of E. LaNave.

analog of the magnetization $M(H, T)$ of a ferromagnet depending on magnetic field H and temperature T only through the correlation length ξ. Specifically, for both models it appears that D follows a general power-law relation of the form

$$D/T \sim (f_{\text{diff}})^{\alpha}, \tag{1}$$

for roughly two decades in f_{diff} and three decades in D/T. For the water model, $\alpha \approx 2$ while for the silica model it appears that $\alpha \approx 1.3$. In the case of silica, the identical functional form describes the relationship between D and f_{diff} both above and below $T_\times$, showing that while the T dependence of both D and f_{diff} is sensitive to the microscopic mechanisms controlling the dynamics, the fragile-to-strong transition does not affect the relation between D and f_{diff}. The exponent value $\alpha = 2$ found for water has recently been theoretically interpreted.[104]

In summary, then, two different dynamical mechanisms affect the slowing down of the dynamics in supercooled states:[98]

(i) In the weakly supercooled region, the slowing down of the dynamics arises from the progressive reduction in the number of directions where free exploration of configuration space is possible. The system is always located close to a multi-dimensional ridge between different basins,

and the time scale of the long-time dynamics is set by the time required to probe one of the free directions. In this range of T, the diffusion is not limited by the presence of energy barriers that must be overcome by thermally activated processes, but is controlled by the limited number of directions leading to different basins along almost constant potential energy paths. Furthermore, the number of free directions completely determines the value of D, independent of the thermodynamic parameters T and ρ.

(ii)   Close to T_{MCT}, the system starts to sample regions of configuration space that have no free directions. The change in the dynamics above and below T_{MCT} can be viewed as a change in the properties of the potential energy landscape sampled in equilibrium, from configurations always close to a ridge of progressively lower and lower dimension to configurations far from any ridge.[105, 106] Below T_{MCT}, the system must go close to the ridge and then select the right direction. The search for the ridge below T_{MCT}, i.e., the search for a rare event, can be probably described as an activated process, which corresponds to Arrhenius behavior of the diffusion constant.

(iii)   The relation between connectivity and number of local minima in the potential energy landscape—which can be calculated in theoretical models as recently done for the random energy model[107]—may help build on the existing ideas bridging thermodynamics and dynamics.[108]

4. DYNAMICS BELOW THE MODE COUPLING THEORY: ''WHAT MATTERS'' IS COOPERATIVE MOTION

4.1. Introduction

As a supercooled liquid is cooled toward the glassy state, the system is increasingly found near local potential energy minima, called inherent structure configurations.[91] In this description, in the glassy state, the system is localized in one of the potential energy basins.[103, 109–111] While such a picture of liquid dynamics is difficult to verify experimentally, computer simulation offers an excellent opportunity to explore these ideas. For a pre-defined liquid potential, a liquid trajectory can be generated via molecular dynamics simulation and the local potential energy minima can be evaluated by an energy minimization method.[91] With this procedure, the motion in phase space is converted into a minimum-to-minimum trajectory, or *inherent structure trajectory*. A general picture of the system moving among a set of basins surrounding the multitude of local minima has evolved. More specifically, simulations have shown that both the depth

of the minima sampled by the system, as well as the number of these minima, decrease on cooling. [111, 112]

The description of the real motion of the system as an inherent structure trajectory becomes a powerful way of separating the vibrational contribution, responsible for the thermal broadening of instantaneous measurements from the slow structural component. [113] Such an approach becomes even more powerful below T_{MCT}, since most of the instantaneous configurations are far from saddles, making correlation functions calculated from the inherent structure trajectory fully account for the α-relaxation dynamics. [109]

4.2. Results

Recent results [114] are based on molecular dynamics simulations of the SPC/E model [115] of water for 216 molecules, at fixed density $\rho = 1$ g/cm^3. The numerical procedure is described in ref. 59. The trajectories are analyzed at $T = 180$ K, and the mode coupling temperature for this density is $T_{MCT} = 193.6$ K, [59] so the system is in the deep supercooled liquid state. At this temperature, the diffusion coefficient is four orders of magnitude smaller than its value at $T = 300$ K and only a few molecules move significantly (with displacements larger than 0.025 nm) at each simulation time step.

To aid in understanding the distribution of the displacements during the IS changes, Fig. 5(a) shows the displacements u of all 216 individual molecules for a typical inherent structure transition. In fact, there is a relatively small set of molecules with a large displacement. A snapshot of the eight molecules with the largest displacement is shown in Fig. 6. Interestingly, this set of molecules forms a cluster of bonded molecules. Indeed, for all cases studied, the set of molecules which displace most forms a cluster of bonded molecules. The observed clustering phenomenon characterizes the inherent structure transitions in water and can be interpreted as the analog of the string-like motion observed in simple atomistic liquids, [109] connected to the presence of dynamical heterogeneities. [116–119] Similar results were found by Ohmine *et al.* using the TIP4P and TIPS2 models for water. [120]

To characterize the distribution of individual molecular displacements between different inherent structures more carefully, Fig. 5(b) shows the distribution of displacements u of the oxygen atoms $P(u)$. Note that $P(u)$ was previously studied by Schrøder *et al.* for a binary Lennard-Jones mixture. [109]

Analysis of the changes in hydrogen bond connectivity associated with inherent structure changes reveals that these transitions are associated with the breaking and reformation of hydrogen bonds.
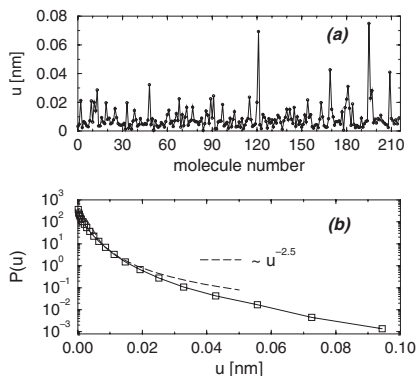
Fig. 5.   (a) Displacement of each of the 216 molecules during the course of a transition from one inherent structure to another. (b) Distribution of displacements u of the oxygen atoms between inherent structure changes, $P(u)$, sampled along a 30 ns trajectory in 20,000 inherent structure changes. The exponential tail of $P(u)$, with a characteristic length of about 0.02 nm, is mostly due to the highly mobile molecules, while the power law with exponent 2.5 would correspond to an ''elastic'' response of the system to these highly mobile molecules.[123] Courtesy of N. Giovambattista.
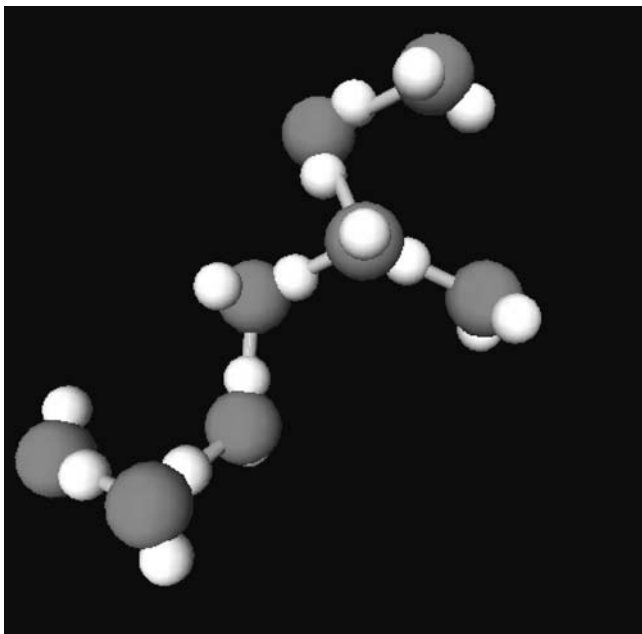

Fig. 6.   Snapshot of the system in one inherent structure. Only the eight molecules with displacement larger than 0.025 nm [Fig. 3(a)] are shown here. Hydrogen-bonded molecules are connected by tubes. Note that all 8 molecules are nearby and form a cluster, which unlike the Lennard–Jones case, are bounded and less string-like. Courtesy of N. Giovambattista.

Reference 114 further shows that the transitions associated with an increase in the energy correspond to the breaking of linear bonds and to the simultaneous formation of bifurcated bonds.[121, 122] Similarly, the transitions associated with a decrease in the energy correspond to the breaking of bifurcated bonds and to the simultaneous formation of linear bonds. This result supports the hypothesis that the linear to bifurcated transition can be considered as an elementary step in the rearrangement of the hydrogen bond network.

ACKNOWLEDGMENTS

REFERENCES

1. P. G. Debenedetti, *Metastable Liquids* (Princeton University Press, Princeton, 1996).
2. P. G. Debenedetti and H. E. Stanley, The novel physics of water at low temperatures, *Phys. Today* (submitted).
3. M.-C. Bellissent-Funel, ed., *Hydration Processes in Biology: Theoretical and Experimental Approaches* (IOS Press, Amsterdam, 1999).
4. O. Mishima and H. E. Stanley, Nature **396**:329 (1998).
5. P. Ball, *Life's Matrix: A Biography of Water* (Farrar Straus and Giroux, New York, 2000).
6. V. Brazhkin, S. V. Buldyrev, V. Ryzhov, and H. E. Stanley, eds., *New Kinds of Phase Transition Phenomena*, Proc. Volga River NATO Advanced Research Workshop (Kluwer, Dordrecht, 2002).
7. H. E. Stanley, *J. Phys. A* **12**:L329 (1979).
8. H. E. Stanley and J. Teixeira, *J. Chem. Phys.* **73**:3404 (1980).
9. A. Geiger and H. E. Stanley, *Phys. Rev. Lett.* **49**:1749 (1982).
10. L. Bosio, J. Teixeira, and H. E. Stanley, *Phys. Rev. Lett.* **46**:597 (1981).
11. R. L. Blumberg, H. E. Stanley, A. Geiger, and P. Mausbach, *J. Chem. Phys.* **80**:5230 (1984).
12. E. Shiratani and M. Sasai, *J. Chem. Phys.* **108**:3264 (1998).
13. P. H. Poole, F. Sciortino, U. Essmann, and H. E. Stanley, *Nature* **360**:324 (1992); *Phys. Rev. E* **48**:3799 (1993); F. Sciortino, P. H. Poole, U. Essmann, H. E. Stanley, Ibid. **55**:727 (1997); S. Harrington, R. Zhang, P. H. Poole, F. Sciortino, and H. E. Stanley, *Phys. Rev. Lett.* **78**:2409 (1997).
14. T. Andrews, *Phil. Trans.* **159**:575 (1869).
15. O. Mishima, H. E. Stanley, *Nature* **392**:164 (1998).

16. O. Mishima, *Phys. Rev. Lett.* **85**:334 (2000).
17. P. W. Bridgman, *Proc. Amer. Acad. Arts Sci.* **47**:441 (1912).
18. L. F. Evans, *J. Appl. Phys.* **38**:4930 (1967).
19. R. S. Smith and B. D. Kay, *Nature* **398**:788 (1999).
20. K. P. Stevenson, G. A. Kimmel, Z. Dohnalek, R. S. Smith, and B. D. Kay, *Science* **283**:1505 (1999).
21. M.-C. Bellissent-Funel, *Europhys. Lett.* **42**:161 (1998).
22. M.-C. Bellissent-Funel, L. Bosio, *J. Chem. Phys.* **102**:3727 (1995).
23. A. K. Soper and M. A. Ricci, *Phys. Rev. Lett.* **84**:2881 (2000).
24. M. A. Ricci and A. K. Soper, *Phys. A* **304**:43 (2002).
25. O. Mishima, *J. Chem. Phys.* **100**:5910 (1994).
26. P. H. Poole, F. Sciortino, T. Grande, H. E. Stanley, and C. A. Angell, *Phys. Rev. Lett.* **73**:1632 (1994).
27. C. F. Tejero and M. Baus, *Phys. Rev. E* **57**:4821 (1998).
28. F. W. Starr, S. Sastry, E. La Nave, A. Scala, H. E. Stanley, and F. Sciortino, *Phys. Rev. E* **63**:041201 (2001).
29. A. Scala, F. W. Starr, E. La Nave, H. E. Stanley, and F. Sciortino, *Phys. Rev. E* **62**:8016 (2000).
30. M. Yamada, S. Mossa, H. E. Stanley, and F. Sciortino, *Phys. Rev. Lett.* **88**:195701 (2002); cond-mat/0202094.
31. S. Sastry, P. G. Debenedetti, F. Sciortino, and H. E. Stanley, *Phys. Rev. E* **53**:6144 (1996).
32. H. Tanaka, *J. Chem. Phys.* **105**:5099 (1996).
33. H. Tanaka, *Nature* **380**:328 (1996).
34. P. A. Netz, F. W. Starr, H. E. Stanley, and M. C. Barbosa, *J. Chem. Phys.* **115**:344 (2001).
35. F. W. Starr, C. A. Angell, and H. E. Stanley, cond-mat/9903451.
36. P. C. Hemmer and G. Stell, *Phys. Rev. Lett.* **24**:1284 (1970).
37. G. Stell and P. C. Hemmer, *J. Chem. Phys.* **56**:4274 (1972).
38. C. K. Hall and G. Stell, *Phys. Rev. A* **7**:1679 (1973).
39. M. R. Sadr-Lahijany, A. Scala, S. V. Buldyrev, and H. E. Stanley, *Phys. Rev. Lett.* **81**:4895 (1998).
40. M. R. Sadr-Lahijany, A. Scala, S. V. Buldyrev, and H. E. Stanley, *Phys. Rev. E* **60**:6714 (1999).
41. A. Scala, M. R. Sadr-Lahijany, N. Giovambattista, S. V. Buldyrev, and H. E. Stanley, *Phys. Rev. E* **63**:041202 (2001).
42. A. Scala, M. R. Sadr-Lahijany, N. Giovambattista, S. V. Buldyrev, and H. E. Stanley, *J. Stat. Phys.* **100**:97 (2000).
43. E. A. Jagla, *Phys. Rev. E* **58**:1478 (1998).
44. E. A. Jagla, *J. Chem. Phys.* **111**:8980 (1999).
45. E. A. Jagla, *Phys. Rev. E* **63**:061509 (2001).
46. G. Franzese, G. Malescio, A. Skibinsky, S. V. Buldyrev, and H. E. Stanley, *Nature* **409**:692 (2001).
47. G. Malescio and G. Pellicane, *Phys. Rev. E* **63**:020501 (2001).
48. F. H. Stillinger and T. Head-Gordon, *Phys. Rev. E* **47**:2484 (1993).
49. F. H. Stillinger and D. K. Stillinger, *Phys. A* **244**:358 (1997).
50. T. Head-Gordon and F. H. Stillinger, *J. Chem. Phys.* **98**:3313 (1993).
51. N. Guisoni and V. B. Henriques, *J. Chem. Phys.* **115**:5238 (2001).
52. S. V. Buldyrev, G. Franzese, N. Giovambattista, G. Malescio, M. R. Sadr-Lahijany, A. Scala, A. Skibinsky, and H. E. Stanley, *Phys. A* **304**:23 (2002).
53. F. W. Starr, M.-C. Bellissent-Funel, and H. E. Stanley, *Phys. Rev. E* **60**:1084 (1999).
54. M. Sasai, *Phys.* **285**:315 (2000).

55. S. J. Henderson and R. J. Speedy, *J. Phys. E: Scientific Instrumentation* **13**:778 (1980).
56. J. L. Green, D. J. Durben, G. H. Wolf, and C. A. Angell, *Science* **249**:R649 (1990).
57. H. Tanaka, *J. Chem. Phys.* **105**:5099 (1996).
58. P. Gallo, F. Sciortino, P. Tartaglia, and S.-H. Chen, *Phys. Rev. Lett.* **76**:2730 (1996).
59. F. W. Starr, F. Sciortino, and H. E. Stanley, *Phys. Rev. E* **60**:6757 (1999); F. W. Starr, S. T. Harrington, F. Sciortino, and H. E. Stanley, *Phys. Rev. Lett.* **82**:3629 (1999).
60. J. R. Errington and P. G. Debenedetti, *Nature* **409**:318 (2001).
61. I. I. Vaisman, L. Perera, and M. L. Berkovitz, *J. Chem. Phys.* **98**:9859 (1993).
62. M. W. Mahoney and W. L. Jorgensen, *J. Chem. Phys.* **112**:8910 (2000); *Ibid.* **114**:363 (2001).
63. F. H. Stillinger and A. Rahman, *J. Chem. Phys.* **60**:1545 (1974).
64. J. M. Sorenson, G. Hura, R. M. Glaeser, and T. Head-Gordon, *J. Chem. Phys.* **113**:9149 (2000).
65. P. A. Netz, F. W. Starr, H. E. Stanley, and M. C. Barbosa, *J. Chem. Phys.* **115**:344 (2001); cond-mat/0102196; P. A. Netz, F. W. Starr, H. E. Stanley, and M. C. Barbosa, cond-mat/0201130; P. A. Netz, F. Starr, M. C. Barbosa, and H. E. Stanley, cond-mat/0201138.
66. P. H. Poole, M. Hemmati, and C. A. Angell, *Phys. Rev. Lett.* **79**:2281 (1997).
67. I. Saika-Voivod, F. Sciortino, and P. H. Poole, *Phys. Rev. E* **63**:011202 (2001).
68. E. G. Ponyatovskii, *JETP Lett.* **66**:281 (1997).
69. E. G. Ponyatovskii and O. I. Bakalov, *Mater. Sci. Rep.* **8**:147 (1992).
70. M. Togaya, *Phys. Rev. Lett.* **79**:2474 (1997).
71. J. Glosli and F. H. Ree, *Phys. Rev. Lett.* **82**:4659 (1999).
72. S. Sastry and C. A. Angell (2002) preprint.
73. Y. Katayama, T. Mizutani, W. Utsumi, O. Shimomure, M. Yamakata, and K.-I. Funakoshi, *Nature* **403**:170 (2000).
74. G. Ruocco *et al.*, (2002) preprint.
75. C. A. Angell, (private communication) has pointed out that the fact that the low density liquid phase of phosphorus that participates in a liquid–liquid equilibrium contains tetrahedral molecules, is not of as much significance as originally hoped. There are no third neighbor correlations in P4 phosphorus, which is more like carbon tetrachloride than water in its behavior. The liquid–liquid phase transition line in the phase diagram runs vertical to the *P* axis, instead of nearly horizontal as in the case of water, and the liquid–liquid equilibrium is due to electron redistribution (i.e., chemical bonding changes) rather than molecular packing changes as in the case of water. Such equilibria will likely be found in the future in many cases of molecular liquids subjected to high pressure (simply because polymerized forms occupy less volume)—and molecular shapes in the low pressure phase will be found to be a minor factor. We thank C. A. Angell for sharing his observations with us.
76. C. A. Angell, R. D. Bresel. M. Hemmati, E. J. Sare, and J. C. Tucker, *Phys. Chem. Phys.* **2**:1559 (2000).
77. S. Sastry, P. G. Debenedetti, and F. H. Stillinger, *Nature* **393**:554 (1998).
78. F. Sette, M. H. Krish, C. Masciovecchio, G. Ruocco, and G. Monaco, *Science* **280**:1550 (1998).
79. P. Lunkenheimer, A. Pimenov, and A. Loidl, *Phys. Rev. Lett.* **78**:2995 (1997).
80. W. Götze, *J. Phys.: Cond. Mat.* **11**:A1 (1999).
81. K. Binder *et al.*, in *Complex Behavior of Glassy Systems*, M. Rubí and C. Perez-Vicente, eds. (Springer, Berlin, 1997).
82. W. Kob, *J. Phys.: Cond. Mat.* **11**:R85 (1999).

83. M. Mézard and G. Parisi, *J. Phys.: Cond. Mat.* **11**:A157 (1999).
84. R. Speedy, *J. Chem. Phys.* **110**:54559 (1999).
85. R. Speedy, *J. Chem. Phys. B* **103**:4060 (1999).
86. M. Shultz, *Phys. Rev. B* **57**:11319 (1998).
87. D. C. Wallace, *Phys. Rev. E* **56**:4179 (1997).
88. P. G. Debenedetti and F. H. Stillinger, *Nature* **410**:259 (2001).
89. I. Saika-Voivod, P. H. Poole and F. Sciortino, *Nature* **412**:514 (2001).
90. S. Sastry, *Nature* **409**:164 (2001).
91. F. H. Stillinger and T. A. Weber, *Phys. Rev. A* **28**:2408 (1983).
92. R. O. Davies and G. O. Jones, *Adv. in Phys.* **2**:370 (1953).
93. M. Goldstein, *J. Chem. Phys.* **51**:3728 (1969).
94. T. Keyes, *J. Phys. Chem. A* **101**:2921 (1997).
95. W. Li and T. Keyes, *J. Chem. Phys.* **111**:5503 (1999).
96. T. Keyes, *J. Chem. Phys.* **101**:5081 (1994).
97. J. D. Gezelter, E. Rabani, and B. J. Berne, *J. Chem. Phys.* **107**:4618 (1997).
98. E. La Nave, A. Scala, F. W. Starr, H. E. Stanley, and F. Sciortino, *Phys. Rev. E* **64**:036102 (2001).
99. S. Bembenek and B. Laird, *Phys. Rev. Lett.* **74**:936 (1995).
100. W. Li, T. Keyes, and F. Sciortino, *J. Chem. Phys.* **108**:252 (1998).
101. E. La Nave, A. Scala, F. W. Starr, F. Sciortino, and H. E. Stanley, *Phys. Rev. Lett.* **84**:4605 (2000).
102. E. La Nave, H. E. Stanley, and F. Sciortino, *Phys. Rev. Lett.* **88**:035501 (2002).
103. L. Angelani, G. Ruocco, A. Scala, and F. Sciortino, *Phys. Rev. Lett.* **85**:5356 (2000).
104. M. Sasai, *Proc. International Conference on Slow Dynamics and Glass Transition* (Bangalore, India, 6-10 January 2002).
105. F. Sciortino and P. Tartaglia, *Phys. Rev. Lett.* **78**:2385 (1997).
106. L. Angelani, R. Di Leonardo, G. Ruocco, A. Scala, and F. Sciortino, *Phys. Rev. Lett.* **85**:5356 (2000).
107. T. Keyes, *Phys. Rev. E* **62**:7905 (2000).
108. G. Adam and J. H. Gibbs, *J. Chem. Phys.* **43**:139 (1965).
109. T. B. Schrøder, S. Sastry, J. C. Dyre, and S. C. Glotzer, *J. Chem. Phys.* **112**:9834 (2000).
110. A. Heuer, *Phys. Rev. Lett.* **78**:4051 (1997).
111. F. Sciortino, W. Kob, and P. Tartaglia, *Phys. Rev. Lett.* **83**:3214 (1999).
112. A. Scala, F. W. Starr, E. La Nave, F. Sciortino, and H. E. Stanley, *Nature* **406**:166 (2000).
113. I. Ohmine and H. Tanaka, *Chem. Rev.* **93**:2545 (1993).
114. N. Giovambattista, F. W. Starr, F. Sciortino, S. V. Buldyrev, and H. E. Stanley, *Phys. Rev. E* **65**:041502 (2002).
115. H. J. C. Berendsen, J. R. Grigera, and T. P. Straatsma, *J. Phys. Chem.* **91**:6269 (1987).
116. M. Hurley and P. Harrowell, *Phys. Rev. E* **52**:1694 (1995).
117. W. Kob, C. Donati, S. J. Plimpton, P. H. Poole, and S. C. Glotzer, *Phys. Rev. Lett.* **79**:2827 (1997).
118. C. Donati, J. F. Douglas, W. Kob, S. J. Plimpton, P. H. Poole, and S. C. Glotzer, *Phys. Rev. Lett.* **80**:2338 (1998).
119. B. Doliwa and A. Heuer, *Phys. Rev. Lett.* **80**:4915 (1998).
120. I. Ohmine and S. Saito, *Acc. Chem. Res.* **32**:741 (1999).
121. F. Sciortino, A. Geiger, and H. E. Stanley, *Nature* **354**:218 (1991).
122. F. Sciortino, A. Geiger, and H. E. Stanley, *J. Chem. Phys.* **96**:3857 (1992).
123. J. C. Dyre, *Phys. Rev. E* **59**:2458 (1999).